pISSN 1229-3008 eISSN 2287-6251
Progress in Superconductivity and Cryogenics
Vol.23, No.3, (2021), pp.45~50 https://doi.org/10.9714/psac.2021.23.3.045

Superconducting properties of MgB_2 superconductors *in-situ* processed using various boron powder mixtures

M. O. Kang[a,b,@], J. Joo[b], B.-H. Jun[a], and C.-J. Kim[a,*]

[a]*Advanced 3D Printing Technology Research Division, Korea Atomic Energy Research Institute, Daejeon, Korea*
[b]*School of Advanced Material Science and Engineering, Sungkyunkwan University, Suwon, Korea*

(Received 29 June 2021; revised or reviewed 14 July 2021; accepted 15 July 2021)

Abstract

In this study, the effect of the size of B powder on the critical current density (J_c) of MgB_2 prepared by an *in situ* reaction process was investigated. Various combinations of B powders were made using a micron B, ball-milled B and nano B powders. Micron B powder was reduced by ball milling and the milled B powder was mixed with the micron B or nano B powder. The mixing ratios of the milled B and micron or nano B were 100:0, 50:50 and 0:100. Non-milled micron B powder was also mixed with nano powder in the same ratios. Pellets of (2B+Mg) prepared with various B mixing ratios were heat-treated to form MgB_2. T_c of MgB_2 decreased slightly when the milled B was used, whereas the J_c of MgB_2 increased with increasing amount of the milled B or the nano powder. The used of the milled B and nano B power promoted the formation MgB_2 during heat treatment. In addition to the enhanced formation of MgB_2, the use of the powders reduced the grain size of MgB_2. The use of the milled and nano B powder increased the J_c of MgB_2. The highest J_c was achieved when 100% nano B powder was used. The J_c enhancement is attributed to the high volume fraction of the superconducting phase (MgB_2) and the large grain boundaries, which induces the flux pinning at the magnetic fields.

Keywords: MgB_2, in-situ process, B powder, milling, powder size, grain size, superconducting transition temperature, critical current density, apparent density, phase formation

1. INTRODUCTION

MgB_2 is a promising material that is expected to replace the conventional NbTi superconductors using liquid He, because it has a very high superconductivity transition temperature (T_c) of 39 K [1]. MgB_2 can be cooled to a temperature of 20 K with only a refrigerator without using expensive liquid helium. Therefore, it can be used for MRI medical devices operating at 20 K or superconducting magnets.

MgB_2 is generally synthesized by the reaction of Mg and B powder [2-12]. Synthesized MgB_2 powder or a mixture of (Mg+B) powder is used as a precursor for MgB_2 superconducting wires. The process using the synthesized MgB_2 is called "*ex situ*" process [5-8], whereas the process using a mixture of Mg and B powder is called "*in situ*" process [9-12]. When the latter is used, the critical current density (J_c) of MgB_2 is higher than that of the former, but the level of J_c of MgB_2 in a magnetic field environment is lower than that of NbTi. To the practical applications of MgB_2 it is thus necessary to increase the J_c of MgB_2 at the magnetic fields. To do this, the characteristics of the precursor powders should be carefully controlled.

The melting point (m.p.) of B, which is a raw material for MgB_2, is very high at 2000℃ [13], whereas m. p. of Mg is relatively low at 649℃ [14]. This means that the diffusion of B at temperatures of 600-900℃, which is the synthesis temperature, is very difficult compared to Mg. On the other hand, the diffusion of Mg is very fast because Mg melts at a temperature above 650℃. Consequently, the synthesis reaction of MgB_2 is governed by the diffusion of Mg.

When a small size B powder is used as a raw material (a large number of B powder), therefore, MgB_2 of fine grains can be obtained. The grain boundaries of MgB_2 have been reported to increase the J_c of MgB_2 at the high magnetic fields [15-17]. The grain size of MgB_2 can be reduced as the size of the B powder is controlled.

In this study, the effect of the size of B powder on the J_c of MgB_2 was investigated. Three different B powders of micron B, milled B and nano B were used as raw materials. The micron B (non-milled) was mixed with the milled B at the appropriated ratios, and also the nano B was mixed with the micron B at the same ratios. MgB_2 pellets were prepared using (2B+Mg) powder mixtures by *in situ* reaction process. An apparent density, phase formation and grain size of MgB_2 and the superconducting properties (T_c and J_c) were investigated.

2. EXPERIMENTAL PROCEDURE

2.1. Raw Powders

Nano B (98.5% purity, an average size 100 nm, PAVEZYUM, Turkey), non-milled B (95~97% purity, an

* Corresponding author: cjkim2@kaeri.re.kr
@ Present association: *Clean Process Lab, SEMES Co. Ltd, Cheonan, Korea*

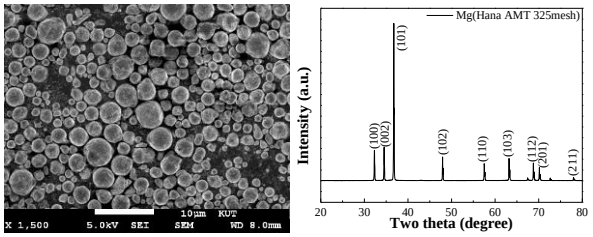

(a) (b)

Fig. 1. (a) FE-SEM image and (b) XRD pattern of Mg used as raw powder.

average size 1 μm, PAVEZYUM, Turkey) and milled B were used as raw powders. Mg powder (99.9% purity, an average size 27.5 μm, Hana ATM, Korea) was used for the reaction with B powders. As can be seen in the SEM image of Fig.1(a) and XRD pattern of Fig.1(b), the used Mg powder is a single phase and has a round shape with particle distribution of 5-10 μm.

The milling procedure carried out for the micron B powder is as follows. Micron B powder and ZrO_2 balls with a diameter of 2 mm were weighed at ratio of 1:20 and were put in a ceramic jar. Toluene (C_7H_8) was used as solvent for milling. The jar was fixed to a body of a planetary milling machine and rotated at a speed of 200 rpm. After 2 h milling, (B+toluene) was separated from balls using a sieve in a wide tray and dried in a vacuum. Drying was performed at 120℃ for 20 h to remove toluene.

Fig.2 shows FE-SEM images of (a) nano B, (b) non-milled B and (c) 2 h milled B. As can be seen in Figs., the nano B is smaller in size than others, the non-milled B powder is composed of plate-like particles of a micron size and the milled B is also composed of plate-like particles but the shape is little irregular due to the local crushing of the particles by milling. In addition, very small particles are observed among the large plate-like particles in the milled B powder. This implies that the size of B powder was reduced by ball milling.

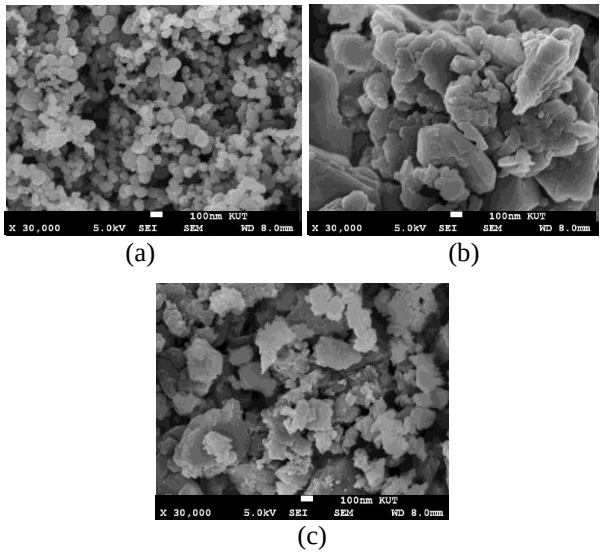

(a) (b)

(c)

Fig. 2. FE-SEM images of (a) nano B, (b) non-milled B and (c) 2 h milled B.

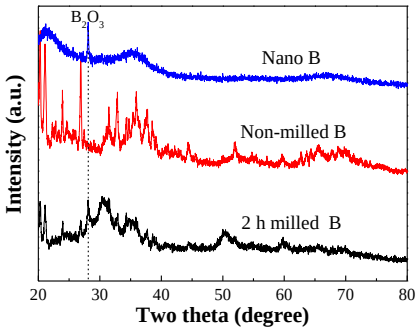

Fig. 3 XRD pattern of nano, non-milled and milled B.

Fig. 3 shows XRD patterns of the three B powders of Figs. 2. In the XRD pattern of the nano B, it is difficult to observed sharp peaks. This is due to the very small grain size of the B powder. In compared with the XRD pattern of nano B powder, many sharp (*hkl*) peaks are observed in the XRD patterns of the non-milled B, which indicates that the micron B has strong crystallinity. On the other hand, the XRD peaks of 2 h milled B was broader than those of the non-milled B. This is owing to the size reduction of B or the increase of an amorphous phase by mechanical milling. It is noticed additionally that the peak of B_2O_3 is observed at $2\theta=28^o$ in both nano and milled B powders. Some of small size B powder is likely to be oxidized during milling or drying process.

2.2. Mixing of powders and Synthesis of MgB_2

MgB_2 was prepared using various combination of B powders by an *in-situ* reaction process using B and Mg powder. The Mg and B powders were weighed to a molar ratio of Mg:B=1:2 and mixed for 30 minutes by hand mixing using a mortar and jar. Three kinds of B powder in various ratios were used. The types and mixing ratios of B precursor powders used in the experiment is summarized in TABLE I.

Powder mixtures of (2B+Mg) were put into a steel mold having a diameter of 10 mm, and then uniaxially pressed with a pressure of 3 tons into pellets. All pellets were sealed in a Ti tube to prevent oxidation of Mg during heat treatment. Heat treatment was performed in an Ar atmosphere at 700℃ for 1 h in a tube furnace. The temperature was raised at a rate of 5℃/min. During the heat treatment, Mg was melt. The melted Mg reacted with the solid B powder to produce MgB_2 according to eq. (1).

TABLE I
BORON POWDER MIXTURES USED AS A PRECURSOR.

Precursor	Ratio of Nano B : Non-milled B
N100	100 : 0
N50-NM50	50 : 50
NM100	0:100

Precursor	Ratio of Nano B : Milled B
N50-M50	50 : 50
M100	0:100

*N: nano, M: milled, NM: non-milled.

$$Mg\ (l) + 2B\ (s) \rightarrow MgB_2\ (s) \quad (1)$$

Here, *l* and *s* represent liquid and solid, respectively. The volume and weight of the pellets before/after heat treatment were measured. The obtained data was used to calculate apparent density. Some of the heat-treated MgB_2 pellets was pulverized into powder, and then X-ray diffraction measurement was performed for the powder samples to analyze the phases formed after heat treatment. Other batches of the heat-treated MgB_2 pellets were cut into a rectangular bars of 3×2×1 mm using a diamond saw. The samples were used to measure the superconducting properties of T_c and J_c. For these samples, MPMS (Magnetic Property Measurement System, Quantum Design, a non-contact magnetic measurement device) was used to estimate the magnetization-temperature *(M-T)* and the magnetization at a constant temperature *(M-B)*. T_c was measured in the range of 32-40 K and the magnetic moment was measured while applying a magnetic field up to 5 T at 5 K and 20 K. The J_c was calculated by Bean's critical model [18] of eq. (2).

$$J_c = 20\Delta M / a(1 - 3a/b) \quad (2)$$

Here, ΔM (M_decreasing field region - M_increasing field region) is magnetization difference at the constant magnetic field, and a and b are parameters related to sample dimension.

3. RESULTS AND DISCUSSION

Fig. 4 shows a histogram of an apparent density vs. a type of used precursor B powder before/after heat treatment. As can be seen in Figs. 4(a), the apparent density of MgB2 pellet decreases regardless of the type of B powder (Nano and non-milled B), the apparent density decreases after heat treatment in all MgB_2 pellets. The decrease of the apparent density means an expansion of pellets. The degree of the pellet expansion is more significant when using nano B powder. The possible cause for the pellet expansion was reported to be the formation reaction of MgB_2 [3, 19]. The out-growth of MgB_2 plates is considered to decrease the pellet density. In this study, more MgB_2 was formed when using nano B powder, which will be discussed later.

The combination of nano and milled B, the density change after heat treatment shows a tendency similar to that of nano/non-milled powder: the density decrease after heat treatment and its dependency on the size of B powder (see Fig. 4(b)). The apparent densities (1.16-1.39 g/cm^3) of the heat treated pellets is smaller than 50% of the theoretical density (2.57 g/cm^3 [19]) of MgB_2. The density results were summarized in TABLE II.

Fig. 5 shows powder XRD patterns of MgB_2 prepared using various B powder mixtures. A major phase in all XRD patterns is MgB_2. Peaks of MgO as a minor phase is also observed. Presence of MgO peak was reported in the sample prepared using powders [20, 21]. It appears to form by the reaction of Mg with oxygen involved in Ar gas or B_2O_3 included in the precursor powder as observed in Fig. 3. The peak intensity of Mg in samples is similar each other, which the formation of MgO was not much influenced by the type of B powder. In addition to the presence of MgO, peaks of unreacted Mg are also observed (see the peaks at 2θ=37°). An amount of unreacted Mg in the pellet prepared using NM100 is maximum, N100 is minimum and M100 is between the two powders. This results indicates that the formation reaction of MgB_2 was activated when using small size B power.

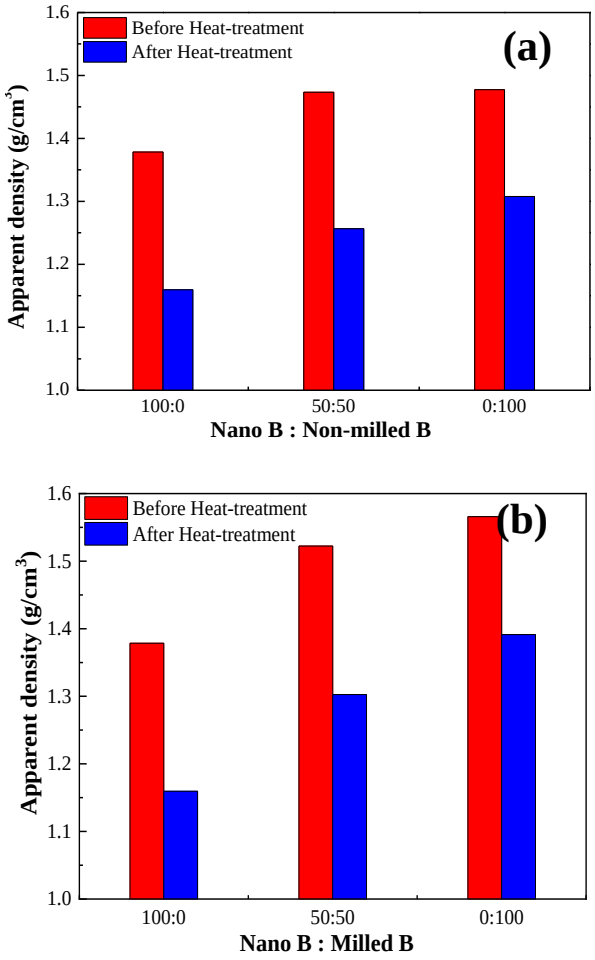

Fig. 4. Histogram of an apparent density of MgB_2 pellets vs. as a ratio of B powders: mixtures of (a) nano B and non-milled B, (b) nano B and milled B.

TABLE II
APPARENT DENSITY AND DENSITY CHANGE (ΔD) BEFORE/AFTER HEAT TREATMENT WITH VARIOUS MIXING RATIO OF BORON POWDERS.

Sample	Apparent density (g/cm^3)		Density change (ΔD) (%)
	before	after	
N100	1.38	1.16	15.9
N50-NM50	1.47	1.26	14.3
N50-M50	1.52	1.30	14.5
NM100	1.48	1.30	12.2
M100	1.57	1.39	11.5

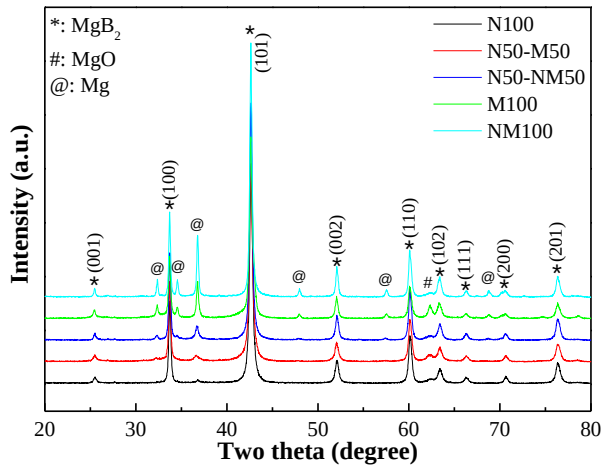

Fig. 5. XRD patterns of MgB_2 prepared using various B powder mixtures.

From the peak intensities of MgB_2, MgO and Mg of Fig. 5, the volume fraction of each phase is calculated and plotted as a function of a powder ratio (Fig. 6). The volume fraction of MgB_2 of the sample using N100 is the highest As for the milled B, the volume fraction increases as a ratio of milled B increase. The volume fraction of MgB_2 prepared using N100 and N50-M50 are about 95% and 90%, respectively, which are much higher than those prepared using N100 and NM100.

In addition to the volume fraction of the each formed phase, the values of FWHM (Full width at half maximum) of (002) and (110) peaks of MgB_2 were measured to calculated the grain size and crystallinity of MgB_2. The grain size was calculated using eq.(3)

$$B\cos\theta = 4\varepsilon\sin\theta + \lambda/L \qquad (3)$$

Where B is FWHM, θ is angle of an incident beam, ε is a strain, λ is a wavelength of the X-ray target and L is grain size. From the FWHM values, we can estimate the defect density or degree of lattice distortion involved in the grain boundaries [22], which induces the flux pinning at magnetic fields.

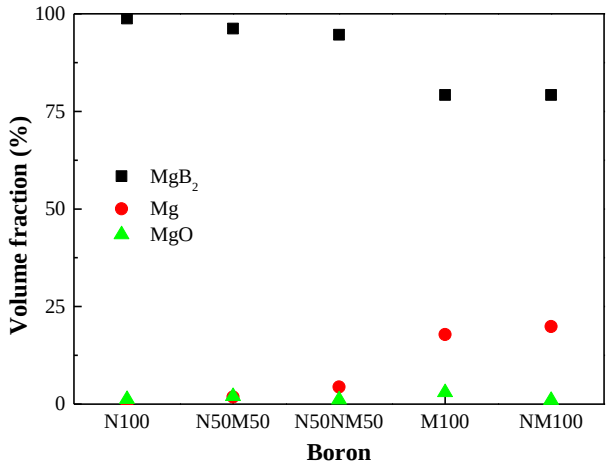

Fig. 6. Volume fraction of MgB_2, Mg and MgO using X-ray diffraction lines.

TABLE III
FWHM OF (002) AND (110) PEAK AND GRAIN SIZE OF MGB_2 OF SAMPLE PREPARED USING VARIOUS B POWDER MIXTURES

Sample	FWHM		Grain size (nm)
	(002)	(110)	
N100	0.400	0.353	37.6
N50-NM50	0.318	0.302	90.6
N50-M50	0.401	0.361	67.0
NM100	0.238	0.285	171
M100	0.293	0.342	73.3

The calculated grains size of MgB_2 was summarized in TABLE III. The highest FWHM value was achieved when using N100. The grain size of MgB_2 of a sample using NM100 is 171 nm and it increase to 73.3 nm as M100 was used. When N100 was used, the smallest grain of 37.6 nm was obtained. This result the use of smaller B powder allows to nucleate many more MgB_2 grains. There are many defects in the grain boundary region and therein the lattice was distorted. They can act as possible pinning centers which traps the magnetic flux [16]. This is the reason why the J_c of MgB_2 was high when a small B power was used as a precursor.

Fig.7 shows FE-SEM images of MgB_2 prepared using (a) N100, (b) N50-M50, (c) M100 and (d) NM100. Plate-shaped MgB_2 grains are observed in all samples. The grain size tends to decrease in the order of NM100, M100, and N100. In samples (b) and (c), small plates are observed among the large plates. The small plates seem to form at the milled B powders. The SEM investigation are in good agreement with the FWHM result of TABLE III.

Fig. 8 shows *M-T* curves and the variation of superconducting transition data of MgB_2 as function of mixing ratio of B. When using NM100 and N100 powder, the superconducting transition ($T_{c,onset}$) is 37.5 K, but when milled B is used, $T_{c,onset}$ is lowered to 37 K. The superconducting transition width (ΔT_c) of NM100 and N100 is 2.0 K, it increases to 3.0 K for M100 and N50-M50.

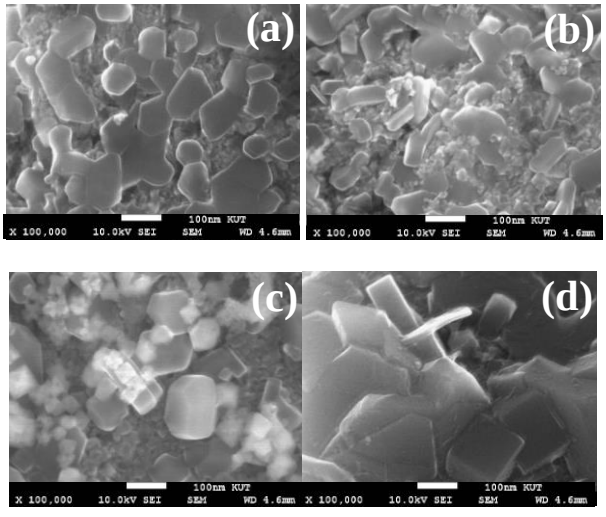

Fig. 7. FE-SEM images of MgB_2 prepared using (a) N100, (b) N50-M50, (c) M100 and (d) NM100.

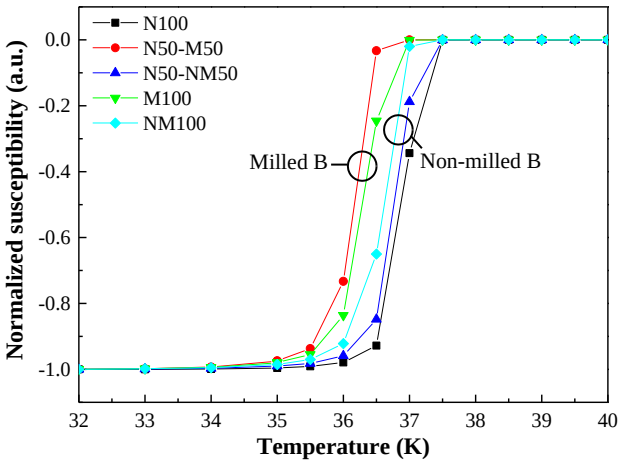

Fig. 8. *M-T* curves of MgB_2 prepared using various B powder mixtures.

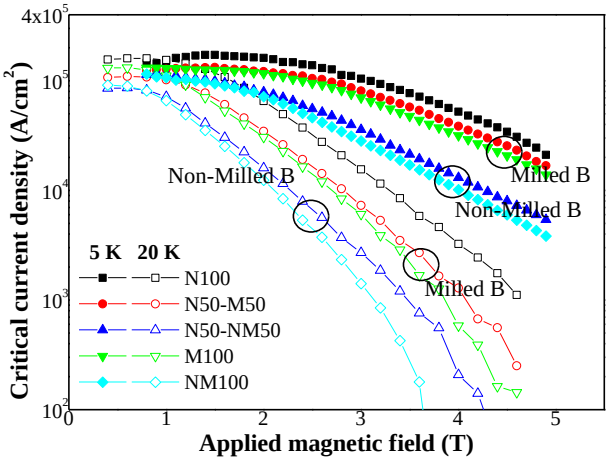

Fig. 9. J_c-B curves of MgB_2 prepared using various B powder ratios.

TABLE IV
SUPERCONDUCTING TRANSITION TEMPERATURE AND TRANSITION WIDTH PREPARED USING VARIOUS B POWDER RATIOS.

Sample	$T_{c,onset}$ (K)	$T_{c,mid}$ (K)	ΔT_c (K)
N100	37.5	36.9	2.0
N50-NM50	37.5	36.8	2.5
N50-M50	37	36.2	3.0
NM100	37.5	36.6	2.5
M100	37	36.3	3.0

The large ΔT_c indicates the decrease in homogeneity of a superconducting phase. The result was summarized in TABLE IV. The similar results were reported in MgB_2 prepared with chemical doping [10] or using milled B powder [15], is considered due to the lattice distortion of MgB_2. The use of the milled B of this study might form MgB_2 containing a relatively large amount of defects (non-superconducting phase).

Fig. 9 shows J_c-B curves at 5 K and 20 K of MgB_2 prepared using various B powder mixtures. As can be seen from J_c-B curves at 5 K, the J_c of N100 is the highest and the J_c of NM100 is the lowest in the entire magnetic field range (0-5 T). In case of the milled powder (M), J_c has an intermediate value of the two powders. Also, J_c is proportional to the content of milled B. The J_c-B results of MgB_2 at 20 K are similar to those at 5 K. The variation of J_c with a type of B powder is owing to the different number of grain boundaries (or defects) of MgB_2.

3. CONCLUSIONS

In this study, the effect of B powder size on the superconducting properties of *in situ* processed MgB_2 was investigated. Various B precursors were prepared by mixing low-purity micron-sized B, milled B, and nano B powder. When milled B and nano B were used as precursor powders and the fraction of the powder was high, the formation reaction of MgB_2 was promoted. The formation reaction of MgB_2 was accompanied by the pellet expansion due to the out-growth of MgB_2 platelets and it was more significant when using smaller B powders. In addition to the high volume fraction of MgB_2, the particle size of MgB_2 decreased as the size of the B powder decreased. The high volume fraction of the superconducting phase (MgB_2) and the reduced particle size of MgB_2 are attributed to the J_c enhancement of MgB_2 at 5 K and 20 K and magnetic field up to 5 T. The J_c was the highest when using 100% nano B powder. The grain boundaries and lattice distortions in MgB_2 seem to enhance the flux pinning capability at high magnetic fields.

ACKNOWLEDGMENT

This work was supported by the National Research Foundation Grant(NRF-2020M2D8A2047959) funded from Ministry of Science and ICT(MSIT) of Republic of Korea.

REFERENCES

[1] J. Nagamatsu, N. Nakagawa, T. Muranaka, Y. Zenitani, and J. Akimitsu, "Superconductivity at 39 K in magnesium diboride," *Nature*, vol. 410, pp. 63-64, 2001.

[2] W. Goldacker, S. I. Schlachter, B. Obst, and M. Eisterer, "*In situ* MgB_2 round wires with improved properties," *Supercond. Sci. Technol.*, vol. 17, pp. S490-S495, 2004.

[3] C. -J. Kim, J. H. Yi, B. -H. Jun, B. Y. You, S. -D. Park, and K. -N. Choo, "Reaction-induced pore formation and superconductivity in *in situ* processed MgB_2 superconductors," *Physica C*, vol. 502, pp. 4-9, 2014.

[4] M. O. Kang, J. Joo, B. -H. Jun, S. -D. Park, C. S. Kim, and C. -J. Kim, "Effect of boron milling on phase formation and the critical current density of MgB_2 bulk superconductors," *Prog. Supercond. Crygen.* vol. 21, pp. 18-24. 2019.

[5] A. V. Pan, S. Zhou, H. Liu, and S. Dou, "Properties of superconducting MgB_2 wires: in situ versus ex situ reaction technique," *Supercond. Sci. Technol.*, vol. 16, pp. 639-644, 2003.

[6] C. U. Jung, M. S. Park, M. S. Kim, J. H. Choi, W. N. Kang, H. P. Kim, and S. I. Lee, "High-pressure sintering of highly dense MgB_2 and its unique pinning properties," *Surr. Appl. Phys.*, vol. 1, pp. 327-331, 2001.

[7] B. A. Glowacki, M. Majoros, M. Vickers, J. E. Evetts, Y. Shi, and I. Mcdougall. "Superconductivity of powder-in-tube MgB_2 wires," *Supercond. Sci. Technol.*, vol. 14, pp. 193-199, 2001.

[8] A. Tampieri, G. Celotti, S. Sprio, R. Caciuffo, and D. Rinaldi, "Study of the sintering behavior of MgB_2 superconductor during hot-pressing," *Physica C*, vol. 400, pp. 97-104, 2004.

[9] E. Martinez, L. A. Angurel, and R. Navarro, "Study of Ag and Cu/MgB_2 powder-in-tube composite wires fabricated by In situ reaction at low temperature," *Supercond. Sci. Technol.*, vol. 15, pp. 1043-1047, 2002.

[10] B. H. Jun and C. J. Kim. "The effect of heat-treatment temperature on the superconducting properties of malic acid-doped MgB_2/Fe wire," *Supercond. Sci. Technol.*, vol. 20, pp. 980-985, 2007.

[11] J. H. Kim, S. X. Dou, J. L. Wang, D. Q. Shi, X. Xu, M. S. A. Hossain, W. K. Yeoh, S. Choi, and T. Kiyoshi, "The effects of sintering temperature on superconductivity in MgB_2/Fe wires," *Supercond. Sci. Technol.*, vol. 20, pp. 448-451, 2007.

[12] A. Yamamoto, J. I. Shimoyama, S. Ueda, Y. Katsura, S. Horii, and K. Kishio, "Improved critical current properties observed in MgB_2 bulk synthesized by low-temperature solid-state reaction," *Supercond. Sci. Tehchnol.*, vol. 18, pp. 116-121, 2004.

[13] G. S. Brady and H. R. Clauser, *Materials Handbook*, 12th ed., vol. 15, pp. 104-105, 1956.

[14] W. Goldacker, S. I. Schlachter, B. Obst, and M. Eisterer, "In-situ MgB_2 round wires with improved properties," *Supercond. Sci. Technol.*, vol. 17, pp. S490-495, 2004.

[15] B. -H. Jun, N. -K. Kim, K. S. Tan, and C. -J. Kim, "Enhanced critical current properties of *in situ* processed MgB_2 wires using milled boron powder and low temperature solid-state reaction," *J. Alloys compd.*, vol. 492, pp. 446-451, 2010.

[16] S. Sugino, A. Yamamoto, J. Shimoyama, and K. Kishio, "Enhanced trapped field in MgB_2 bulk magnets by tuning grain boundary pinning through milling," *Supercond. Sci. Technol*., vol. 28, pp. 055016, 2015.

[17] B. -H. Jun, S. -D. Park, and C. -J. Kim, "Refinement and carbon incorporation effects on the superconducting properties of MgB_2 through wet milling process of low purity boron powder," *J. Alloys compd.*, vol. 535, pp. 27-32, 2012.

[18] C. P. Bean, "Magnetization of High-Field Superconductors," *Rev. Mod. Phys.*, vol. 36, pp.31-39, 1964.

[19] J. H. Yi, K. T. Kim, B.-H. Jun, J. M. Sohn, B. G. Kim, J. Joo, and C. -J. Kim, "Pore formation in '*in situ'* processed MgB_2 superconductors," *Physica C*, vol. 469, no. 15-20, pp. 1192-1195, 2009.

[20] D. N. Kim, B.-H. Jun, S.-D. Park, C.-J. Kim, and H. W. Park, "Effects of the size of Mg powder on the formation of MgB_2 and the superconducting properties," *Prog. Supercond. Crygen.*, vol. 18, pp. 9-14, 2016.

[21] S. H. Kim, W. N. Kang, B.-H. Jun, Y. J. Lee, and C.-J. Kim "Enhanced critical current density of *in situ* processed MgB_2 bulk superconductors with MgB_4 additions," *Prog. Supercond. Crygen.* vol. 19, pp. 36-41, 2017.

[22] P. Scherrer, "Bestimmung der Grösse und der inneren Struktur von Kolloidteilchen mittels Röntgenstrahlen," *Nachr. Ges. Wiss. Göttingen*, vol. 26, pp 98-100, 1918.